Pramāṇa, Vol. 23, No. 5, November 1984, pp. 559–571. © Printed in India.

ΔT-window neutron spectrometer

P S GOYAL, C L THAPER and B A DASANNACHARYA
Nuclear Physics Division, Bhabha Atomic Research Centre, Trombay, Bombay 400 085, India

MS received 13 July 1984

Abstract. A high resolution neutron spectrometer making use of a ΔT-window filter for the analyser and time-of-flight technique for analysing incident neutron energy has been designed. The spectrometer will provide a continuously variable energy resolution ΔE from 40–50 μeV at $\sim$ 5230 μeV. The range of energy transfer allowed is -1450 μeV to $+2950$ μeV and the range of wavevector transfer Q allowed is 0·82–3·06 Å^{-1}. Depending on the resolution used, the counting rates are expected to vary from 28–60 $\times 10^3$ counts/hr if one assumes 10% isotropic elastic scattering from the sample.

Keywords. Neutron spectrometer; window filter; time-of-flight; resolution; intensity, beryllium.

PACS No. 29·30 Hs

1. Introduction

A variety of neutron spectrometers have been built in the past for quasi-elastic and inelastic scattering measurements. They differ, mainly, in the manner of their neutron monochromatisation and/or energy analysis, thus resulting in spectrometers with varying regions of accessible wavevector and energy transfers and differing resolutions. They are either based on principles of crystal diffractometry or time-of-flight spectrometry (Iyengar 1965; Brugger 1965; Buras 1968; Windsor 1981). In crystal spectrometers (Iyengar 1965) which always depend on the use of Bragg Law, $2d \sin \theta = \lambda$, the energy resolution, $\Delta E/E$, depends basically on $\cot \theta \cdot \Delta\theta$ where $\Delta\theta$ is an effective divergence. While a choice of large θ, in order to improve the resolution restricts the available range of wave-vector transfer, Q, a reduction of $\Delta\theta$ beyond a certain value severely affects the intensity. For time-of-flight instruments (Buras 1968; Windsor 1981) the resolution $\Delta E/E = 2\Delta t/t$; this requires increasing the total time-of-flight, t, of the neutrons and reducing Δt, the effective width in the arrival time of neutrons of a given energy at the detector, for achieving a better resolution. Limitations in achieving better resolution arise due to difficulties associated with the use of long flight paths (to get large t) and designing of chopping devices (to get shorter Δt). Consequently, the overall energy resolution of conventional spectrometers is seldom better than about 2%. For example, none of these spectrometers have a resolution better than 100 μeV at 5000 μeV. Special types of instruments like the back-scattering (Alefeld 1969) and spin-echo (Dagleish *et al* 1980) spectrometers, on the other hand, have a resolution ~ 1 μeV, though the allowed region of energy transfer is limited. Thus, there is a need for improving the energy resolution at a given energy, in order to reduce the resolution gap between the 'conventional' and 'special' instruments.

This paper describes a new type of spectrometer, called a 'ΔT-window spectrometer', which attempts to do this. The spectrometer will provide an energy resolution of ~ 40 μeV (continuously changeable to 50 μeV) at ~ 5230 μeV. The allowable range of energy transfer will be from -1450 to $+2950$ μeV. To the best of our knowledge, this will be the first spectrometer with such characteristic parameters. It is possible to improve the resolution down to 20 μeV, in principle, with some changes in design.

The basic idea of the ΔT-window and a spectrometer based on this have been described earlier (Iyengar 1964; Dasannacharya 1981; Goyal *et al* 1982). They are briefly mentioned in §2 for the sake of completeness. The incident beam tailoring required for the spectrometer is described in §3*. The consideration adopted for the design of the sample and ΔT-window analyser systems in order to arrive at the best possible combination of resolution and intensity are given in §4. Using the parameters determined thus, the shape of the resolution function and the anticipated neutron intensity in a typical neutron experiment are evaluated in §5. A preliminary account of this work has been reported earlier (Goyal *et al* 1983).

2. Principle of ΔT-window spectrometer

Figure 1 is a schematic drawing of the spectrometer. A pulse of polychromatic neutrons from the neutron source is allowed to travel a long distance, L_1, before it is incident on the sample. The incident time resolution is $\Delta t/t = V(\Delta t/L_1)$, V being the velocity of the neutrons. Typically, assuming $\Delta t = 100$ μsec, the anticipated full width at half maximum of the SNS (Manning 1978; Taylor 1982) pulse from the liquid hydrogen cold

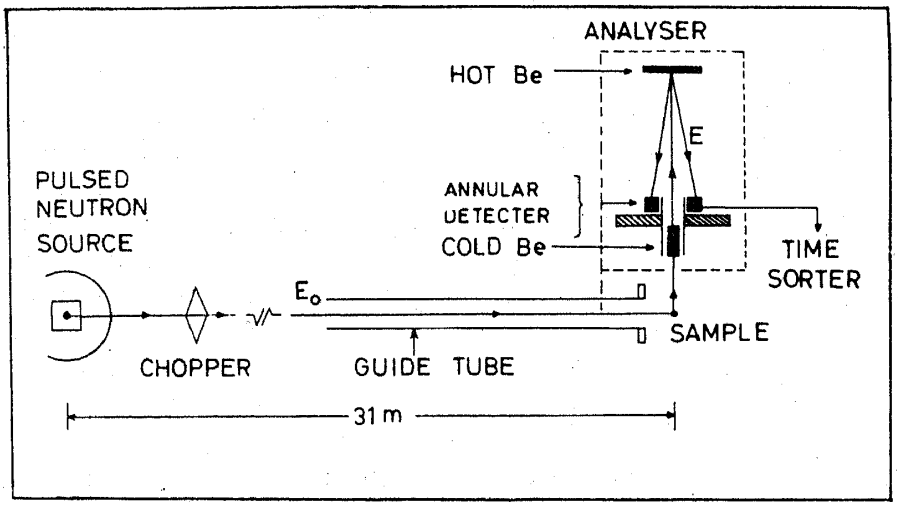

Figure 1. A schematic of the ΔT-window neutron spectrometer with a pulsed source.

* The spectrometer is designed for installation at one of the beams of the Spallation Neutron Source (SNS) at the Rutherford Appleton Laboratory, UK, under a collaboration agreement between the Bhabha Atomic Research Centre (BARC) and the Rutherford Appleton Laboratory. Hence all the design parameters of the instrument are decided with characteristics of SNS in view. The spectrometer has been fabricated at BARC and will be described in detail elsewhere (Dasannacharya *et al* 1984).

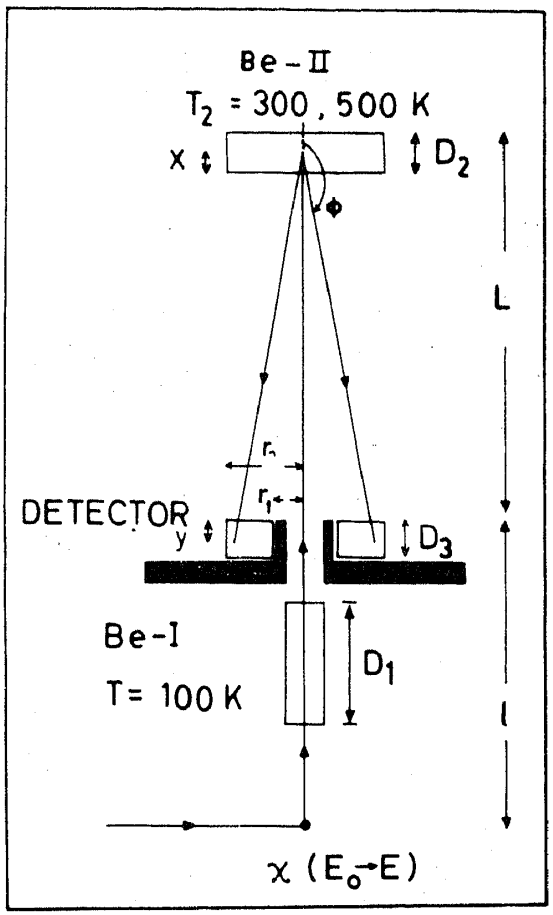

Figure 2. A schematic of ΔT-window analyser indicating the various symbols in the text.

neutron source for $E_0 \sim 5000\ \mu$eV ($V = 1000$ m/sec), one finds, for $L_1 = 31$ m, $\Delta t/t = 0{\cdot}0031$ leading to an energy width $\Delta E_i = 31\ \mu$eV. The pulse of neutrons is scattered by the substance under investigation.

The scattered neutrons are received by the window filter analyser which consists of two beryllium blocks Be(I) and Be(II) kept at temperatures T_1 and T_2 and an annular detector as shown in figures 1 and 2. Most of the neutrons having energies larger than the Bragg cut-off energy, E_{I}, of Be(I) are removed from the scattered beam by Be(I). Out of the transmitted neutrons, those with energy less than E_{II}, the Bragg cut-off energy of beryllium at T_2, pass through Be(II) also. However neutrons in the energy window, Δ, between E_{I} and E_{II}, pass through Be(I), get scattered by Be(II) at backward angles and most of them are detected in the annular detector. Thus, of the neutrons scattered by the specimen, the detector receives only those in a narrow window of width $\Delta = (E_{\text{I}} - E_{\text{II}})$. In general; Bragg cut-off energies E_{I} and E_{II} have finite widths (Thaper *et al* 1984) and the analyser window is not rectangular. In the following discussions, however, the analyser window has been assumed to be rectangular and centred about $\bar{E} = 0{\cdot}5$ $(E_{\text{I}} + E_{\text{II}})$. The width, Δ, of the window can be varied by changing the relative temperatures of the two Be blocks. For $T_1 = 100$ K, Δ varies from 15–40 μeV and $\bar{E}$ from 5229·5–5217·5 μeV* as T_2 is changed from 300–500 K (see figure 3).

* In arriving at these numbers, we have used an effective cut-off energy E_{II} which corresponds to the smallest energy that Be(II) back scatters and is also detected by the annular detector.

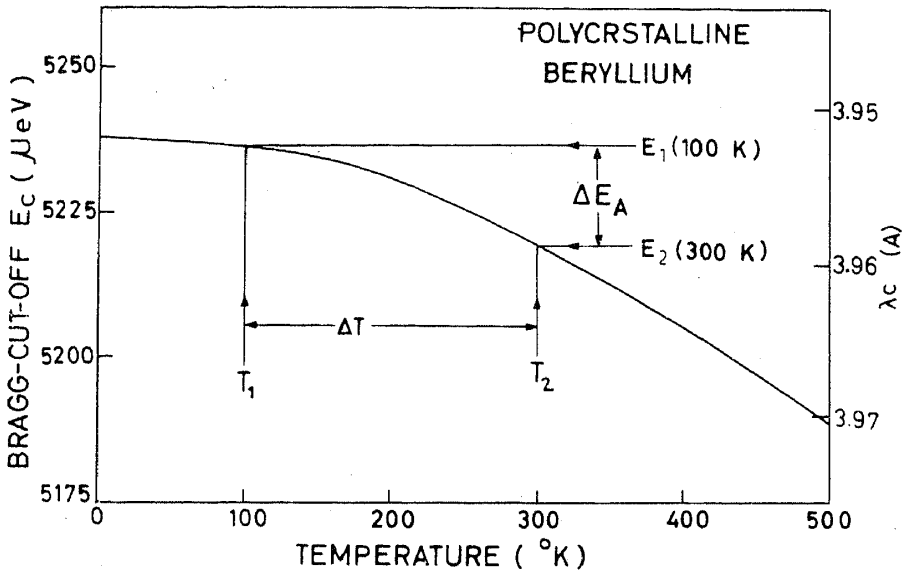

Figure 3. Beryllium cut-off energy as a function of temperature. Lattice parameters are from AIP Handbook 1972.

The scattered neutron spectrum as a function of the energy transfer $\varepsilon = (\bar{E} - E_0)$ is constructed from the measured neutron arrival rate at the detector as a function of the time elapsed since the start of pulse from the source.

3. Incident beam

As already mentioned the sample receives pulses of neutrons from a liquid hydrogen cold neutron source at SNS (Manning 1978) which gives 50 pulses per second. The pulse duration $\Delta t(E_0)$ and the neutron intensity $\phi_0(E_0)$ depend on the energy E_0 of the neutrons. For $E_0 = 5229$ μeV, $\Delta t = 98$ μsec and $\phi_0 = 1{\cdot}84 \times 10^9$ n/μeV/sec/stred (Taylor 1982). Neutron beam from the moderator (100 × 100 mm) is guided onto the sample (42 × 42 mm) at 31 m ($= L_1$) from the moderator using a curved guide tube. To avoid frame overlap (Brugger 1965) a chopper, kept between the moderator and the sample, restricts incident neutron energy between about $\sim$ 2275 μeV and $\sim$ 6675 μeV.

4. Analyser

4.1 *Basic features*

The analyser shown schematically in figure 2 is designed for a situation when Be(I) is at 100 K and the Be(II) temperature can be varied between 300 and 500 K. In addition to geometrical factors, the efficiency of the analyser depends on the transmission, Tr, of Be(I), reflectivity, $\mathscr{R}$, of Be(II) and the efficiency η of the detector for neutrons having energies between E_I and E_{II}. At the same time, the resolution of the analyser, apart from the width of the ΔT-window depends on the thickness of Be(II) and the detector. The design parameters of the analyser have been arrived at to obtain the maximum possible intensity consistent with an analyser resolution compatible with the incident beam resolution.

First, the length of Be(I) was chosen to be 150 mm. At 100 K, this transmits 92% neutrons in the energy region of the window. At the same time it effectively removes most of the neutrons with energies larger than E_I, giving a transmission of 0·15 for $E_1 < E < 6390\ \mu$eV and $< 0{\cdot}001$ for $E > 6390\ \mu$eV.

In a time-of-flight instrument the detector contributes an uncertainty in time-of-flight proportional to its thickness. At the mean energy of the window the detector contribution is about 0·3 μeV/mm. The thickness of the detector, which is a $B^{10}F_3$ gas (95% B^{10}) counter filled at one atmosphere pressure, is 40 mm. This gives an efficiency, $\eta = 0{\cdot}59$ at 5229 μeV and contributes about 13 μeV to the analyser resolution.

In order to arrive at the thickness of Be(II), reflectivity of Be for the relevant condition was calculated (see Appendix). In the energy region of interest the reflectivity, $\mathscr{R}$, of a 50 mm thick block of beryllium is 30% at 300 K and 17·5% at 500 K. The contribution of this to the resolution will be similar to that of the window and the detector and hence this thickness was chosen. It may be noted from the figure in Appendix that beyond this thickness the rate of increase in reflectivity is low.

Now, the inner and outer radii r_1 and r_2 of the detector, radii r and R of Be(I) and Be(II) and distances, l, from the sample to the detector and, L, from the end of the detector to Be(II) (see figure 2) are decided on the basis of the following requirements: (i) Full incident beam size (42 × 42 mm) should be used. (ii) A minimum sample environment area of 500 mm dia around the centre of the sample has to be provided. (iii) Space (200 mm dia) for cryostat for 150 mm long Be(I) to be provided. (iv) Space (~ 140 mm) for adequate shielding between Be(I) and the detector should be given. (v) Adequate shielding ($\simeq$ 10 mm thick) in the inner hole of the detector is necessary. (vi) Adequate size of Be(II) should be chosen so that it receives the full beam that emerges from the central hole in the detector. (vii) Adequate size of the detector should be provided so that it collects neutrons of energies up to E_I on being Bragg scattered from Be(II).

For given thickness of Be(I), Be(II) and the detector, the figure of merit F, of the analyser is:

$$F = \frac{1}{4\pi}\left(\frac{\pi r^2}{l^2}\right)(1-P), \tag{1}$$

where $P = [r_1/L \tan(\pi - \phi)]^2$ is the fraction of nearly back-scattered neutrons which are not received by the detector because of the central hole. Here ϕ is the angle through which E_I neutrons are Bragg scattered by $(10\bar{1}0)$ planes of Be(II). The above expression for the figure of merit assumes that R and r are large enough to meet requirements (vi) and (vii). The design optimization of the analyser involves a suitable choice of parameters r_1, r_2, r, R, l and L which not only meet the above mentioned requirements but also give an optimum F value.

The diameter $2r$, of Be(I) is chosen to be 50 mm to match the size of the incident beam. In view of this and in view of (5), the inner diameter, $2r_1$, of the detector is chosen to be 70 mm. Requirements (ii)–(iv) dictate a minimum value of 630 mm for l. To find an optimum R value, the figure of merit F was calculated as a function of R for l = 630 mm, and is shown in figure 4 for a situation when $T_1 = 100$ and $T_2 = 300$ K. From this, a value of $R = 80$ mm, beyond which F increases very slowly, has been chosen. For this R, (vi) and (vii) suggest that $L = 693$ mm and $r_2 = 100$ mm. Table 1 gives a summary of physical design parameters of the analyser.

It may be mentioned here that a distance of $L = 693$ mm between the detector and

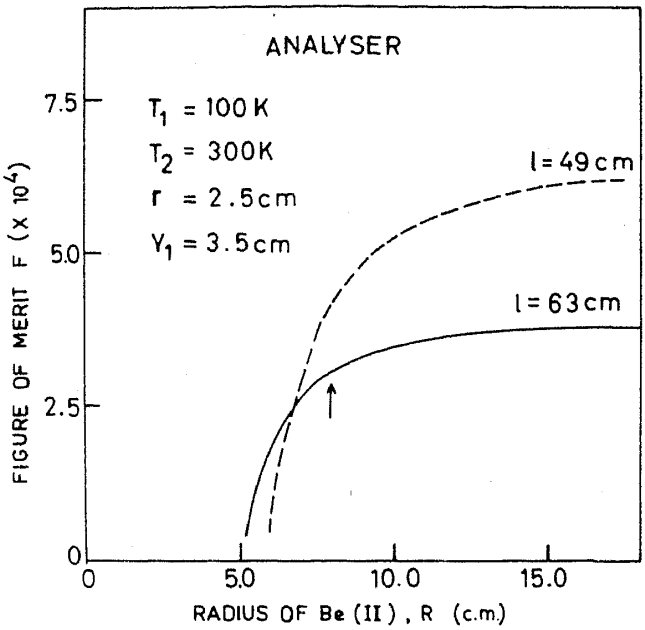

Figure 4. Figure of merit of the ΔT-window analyser as obtained using (1). Arrow indicates the chosen diameter for Be(II).

Be(II) is suitable only when $T_1 = 100$ and $T_2 = 300$ K. When Be(II) is heated to change the spectrometer resolution, the L value should be decreased to meet requirement (vii). For example, for $T_2 = 500$ K, the appropriate L value is 390 mm. Hence, a provision has been made to vary L between 350 mm and 700 mm.

The figure of merit F for the two configurations ($T_2 = 300$, $L = 693$ mm and $T_2 = 500$ K, $L = 390$ mm) discussed above, will be the same ($= 3{\cdot}07 \times 10^{-4}$). The mean energies and the energy windows of the analyser, will however be different in the two cases. For example, when $T_1 = 300$ K the detector collects neutrons in the energy region 5223–5236 μeV (window of 13 μeV) and the mean energy $\bar{E}$ is 5229·5 μeV. On the other hand, when $T_2 = 500$ K the energy window has a width of ~ 37 μeV (5199–5236 μeV) and the mean energy is 5217·5 μeV.

The spectrometer is provided with two analyser arms. The scattering angle can be varied from 30–150° corresponding to wave-vector transfer Q region of 0·82–3 Å^{-1}. The scattering angle has an opening of $\pm 2{\cdot}27°$ for each detector. This gives a wave vector transfer resolution $\Delta Q/Q$ of 7·5% at $Q = 0{\cdot}82$ Å^{-1} and 1% at $Q = 3$ Å^{-1}.

4.2 *Additional features of the spectrometer*

In one of the analyser arms, Be(II) of 200 mm diameter has been used. The spectrometer also has a provision to vary l between 490 and 690 mm. In normal geometry, when a space of 500 mm dia is provided at the sample table, these additional features are not of much help. However, at times, whenever a smaller space around the sample table is acceptable, the additional features can be exploited to gain intensity by choosing a configuration different from those described above. Table 2 gives the figure of merit F for some of the possible configurations allowed by the spectrometer. It is seen that configurations IV and V gives 65% higher intensity compared to configurations I and II respectively without affecting the resolution.

Table 1. Characteristic features of physical design of the analyser.

Beryllium (I)

Radius $r = 25$ mm
Length $D_1 = 150$ mm
Temperature $T_1 = 100$ K
Transmission at 100 K $= T_r = 0{\cdot}92$ for $5219 < E < 5236$ μeV
$= 0{\cdot}15$ for 5236 μeV $< E < 6390$ μeV
$< 0{\cdot}001$ for $E > 6390$ μeV.

Beryllium (II)

Radius $R = 80$ mm in Arm I
$= 100$ mm in Arm II
Thickness $D_2 = 50$ mm
Temperature $T_2 =$ Variable (300–500 K)
Reflectivity of Be for 5229 μeV neutrons $= 0{\cdot}30$ for $T_2 = 300$ K
$= 0{\cdot}175$ for $T_2 = 500$ K

Detector

Gas $= BF_3$ (95% enrichment of B^{10})
Gas pressure $= 750$ mm of mercury column
Thickness $D_3 = 40$ mm
Inner radius $r_1 = 35$ mm
Outer radius $r_2 = 100$ mm
Calculated efficiency $= \eta = 0{\cdot}59$ for 5229 μeV neutrons.

Distances

Sample-Detector distance $l =$ Variable (490–690 mm)
Detector-Be(II) distance $L =$ Variable (350–700 mm)
Space around sample table = Variable (220 mm dia to 620 dia).

Table 2. Allowed configurations on the spectrometer for $T_1 = 100$ K.

Configuration	l (mm)	T_2 (K)	R (mm)	L (mm)	Figure of merit $F(\times 10^4)$	Gain compared to normal geometry
I (normal)	630	300	160	693	3·07	1·0
II (normal)	630	500	160	390	3·07	1·0
III	490	300	160	540	4·16	1·35
IV	490	300	200	693	5·08	1·65
V	490	500	160/200	390	5·08	1·65

5. Resolution and intensity

The energy resolution of the spectrometer depends upon the incident pulse shape $\rho(t', E_0)$, channel width, $\Delta\tau$, of the time sorter, uncertainty in flight path and edges E_I and E_{II} of the window filter. If the proton pulse from the accelerator is incident on the target at $t = 0$, neutrons of energy E_0 may start from the moderator at time t' depending on the pulse shape. The main sources of uncertainty in flight path are thickness D_2 and D_3 of Be(II) and the detector. Neutrons may be Bragg reflected at any depth in Be(II) and similarly they may be detected at any depth in the detector. The uncertainty in the flight path arising from the number of reflections the neutron suffers in the guide tube is negligible ($\sim$ 0·3 mm). The small uncertainty ($\sim$ 10 mm) in the flight path that arises because of the sample size and finite divergences of the incident and the scattered beams is also neglected. In the following we write an expression for the intensity $I(t)\Delta\tau$ of neutrons reaching the time sorter during a time interval $\Delta\tau$ between $(t - \frac{1}{2}\Delta\tau)$ and $(t + \frac{1}{2}\Delta\tau)$ when a sample having differential scatterng cross-section $\chi(E_0 \to E)$ is kept on the sample-table. When $\chi(E_0 \to E) = \delta(E_0 - E)$, this expression will give the shape of the resolution function.

Let us assume that neutrons of energy E_0 start from the moderator at time t'. These neutrons get scattered at the sample position and change their energy to E. Let us further assume that scattering from the sample is isotropic. Depending on the value of E and the solid angle $\Delta\Omega$ ($= \pi r^2/l^2$) that the analyser substends at the sample position, a part of these neutrons will pass through Be(I) of the analyser. After passing through Be(I), let us assume that these neutrons are scattered in Be(II) at a depth between x and $x + dx$ and a part (decided by geometrical factors) of them are detected in the detector at a depth between y and $y + dy$. Neutrons can reach the detector after suffering either Bragg scattering (elastic) or an inelastic scattering process ($E \to E'$) in Be(II). Bragg scattered neutrons give the real signal. Inelastically (non-Bragg) scattered neutrons give rise to a diffuse background. If t'' is the time at which neutrons are counted in the detector, then it can be shown that

$$I(t)\Delta\tau = (2\gamma_c)^2 \frac{A_s}{A_m} \int dE_0\, \phi_0(E_0) \int dt'\, \rho(t', E_0) \times \int dE \frac{\Delta\Omega}{4\pi} \chi(E_0 \to E) \cdot \times \int_0^{D_2} dx \int_0^{D_3} dy \int dE' f(E, E', E_I, E_{II}, x, y) \int f(t'')\, dt'', \tag{2}$$

where

$$\int f(t'')\, dt'' = 1 \text{ if } (t - \tfrac{1}{2}\Delta\tau) < t'' < (t + \tfrac{1}{2}\Delta\tau)$$
$$= 0 \text{ otherwise} \tag{3}$$

γ_c, A_m and A_s are the critical angle (= 24′ for 5229 μeV neutrons for nickel coated tube), moderator area and the sample area respectively. $\phi_0(E_0)$ is the number of neutrons emitted by the moderator per unit time and per unit energy interval per unit solid angle at E_0. $\rho(t', E_0)$ is the pulse shape of neutrons having energy E_0. $\chi(E_0 \to E)$ is the double differential scattering cross-section of the sample. We have assumed $\chi(E_0 \to E)$ to be isotropic. When a neutron of energy E enters the analyser, $f(E, E', E_I, E_{II}, x, y)$ gives the probability that it will pass through Be(I), get scattered in Be(II) at a depth of x, change its energy to E' ($E' = E$ for Bragg scattering) and then get counted in the detector at a depth of y. We will not give here the lengthy expression for $f(E, E', E_I, E_{II}, x, y)$. This

function is mainly decided by the Bragg and inelastic scattering characteristics of Be(II) and the counting efficiency of the detector. In general, the function f depends on the geometrical parameters (r_1, r_2, L) also. Depending on the geometry, only a fraction of neutrons scattered by Be(II) reach the detector. The time t'' at which neutrons are counted in the detector is given by

$$t'' = t' + \frac{CL_1}{\sqrt{E_0}} + \frac{C(l+L-0{\cdot}5D_2+x)}{\sqrt{E}} + \frac{C(L-0{\cdot}5D_2+x+y)}{\sqrt{E'}}. \tag{4}$$

Here $C = 72290$, when distances are in meters and energy in μeV.

The time of flight distribution $I(t)\Delta\tau$ as a function of energy transfer $[\varepsilon = (\bar{E} - E_0)]$ have been evaluated numerically using (2)–(4) assuming incident pulse to be instantaneous, $\rho(t', E_0) = \delta(t')$, a delta function for all values of E_0 and assuming 10 % elastic scattering from the sample $[\chi(E_0 \to E) = 0{\cdot}1\delta(E - E_0)]$. Results for $T_1 = 100$, and $T_2 = 300$ and 500 K are shown in figure 5 for configurations IV and V of table 2. The relevant cross-sections of Be used have been taken from BNL report (Hughes and Harvey 1955) (Also see Appendix).

In the above calculations, diffuse background contribution to $I(t)\Delta\tau$ has been calculated in an approximate way. To avoid integration over E' and to simplify the geometrical corrections, non-Bragg scattering from Be(II) has been assumed to be isotropic* and elastic. In view of the fact that transmission of Be(I) increases sharply at

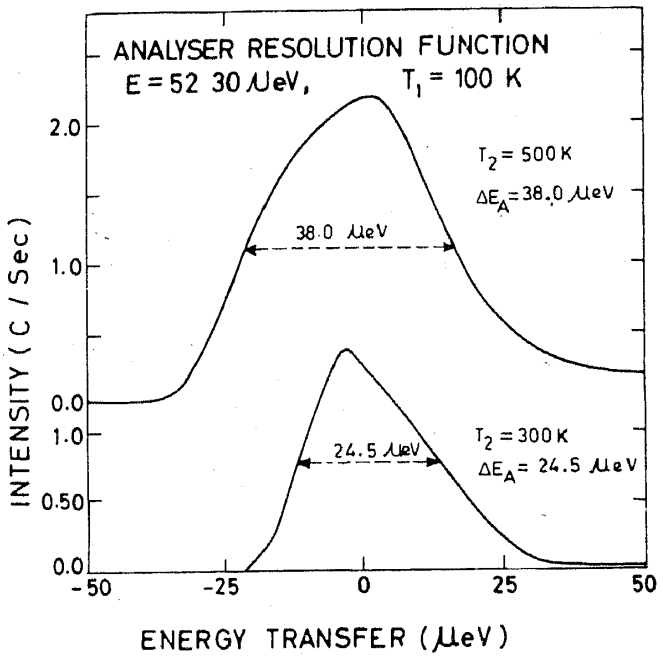

Figure 5. Calculated resolution function of the analyser for different temperatures of Be(II), when Be(I) is at 100 K.

* In general non-Bragg scattering from Be is inelastic and is not isotropic. In this case, neutron energy E ($\sim E_{II}$) is much smaller than the temperature T_2 of Be and Debye temperature of Be. Thus during non-Bragg scattering, neutrons are expected to gain in energy leading to $E' > E_{II}$. Because of a sudden increase in Bragg scattering cross-section of Be at $E = E_{II}$, inelastic scattering in Be(II) is often followed by a Bragg scattering. Thus even if the inelastic scattering is not isotropic, the two scatterings tend to make it isotropic.

$E = E_1$ and because non-Bragg scattering in Be(II) has also been assumed to be elastic, there is a sharp increase in the background in the region of zero energy transfer (see figure 5, the background on energy loss side is higher as compared to that on the energy gain side). In more exact calculations where the spectra of E' is decided by the phonon density of states of Be(II), the diffuse background shown in figure 5 will get redistributed. It will decrease on the energy loss side and increase on the energy gain side. The background on the energy loss side in figure 5 gives an upper limit. We note that diffuse background is 10% of peak intensity for $T_2 = 500$ K and 2% for $T_2 = 300$ K.

When the sample scatters 10% of the neutrons, the integrated counting rates for the two temperatures of Be(II) are 28×10^3 and 60×10^3 counts/hr for configurations IV and V of table 2. It may be noted that for other configurations the intensities will be smaller by an amount, decided by the change in the value of the figure of merit F (see table 2).

As the incident pulse has been assumed to be instantaneous and the scattering to be elastic, figure 5 gives the shapes of the resolution function for $T_2 = 300$ and 500 K of the analyser alone. The shape of the overall spectrometer resolution will be calculated when the incident pulse shape $\rho(t', E_0)$ is known. It may be noted however that calculated analyser resolution ΔE_A (FWHM) are 24·5 and 38 μeV for $T_2 = 300$ and 500 K. Assuming pulse width Δt (FWHM) to be 98 μsec, incident resolution ΔE_i comes to be 31 μeV. By root mean square addition of widths, this gives the spectrometer resolution ΔE to be 39·5 and 49 μeV for the two temperatures of Be(II). We note that intensity more than doubles with only a marginal (24%) deterioration of resolution when T_2 is changed from 300 to 500 K. Table 3 summarizes the characteristic features of the spectrometer.

Table 3. Characteristic features of the ΔT-window neutron spectrometer.

Parameters \ Temperatures	$T_1 = 100$ K	
	$T_2 = 300$ K	$T_2 = 500$ K
Incident resolution ΔE_i	31·0 μeV	31·0 μeV
Analyser resolution ΔE_A	24·5 μeV	38·0 μeV
Spectrometer resolution ΔE	39·5 μeV	49·0 μeV
Spectrometer resolution $\Delta E/E$	0·755%	0·937%
Typical counting rate/hr	28000	60000
Signal/background at peak	50	10

Mean Energy $\bar{E} = 5229{\cdot}5$ μeV for $T_2 = 300$ K
$= 5217{\cdot}5$ μeV for $T_2 = 500$ K
Range of $\varepsilon = -1450$ μeV to $+2950$ μeV

Scattering angle range = 30–150°
Range of $Q = 0{\cdot}82$–3.06 Å^{-1}
Wavevector transfer resolution $\Delta Q/Q = 7{\cdot}5$–1%.

6. Summary

A high resolution ΔT-window neutron spectrometer which makes use of a window filter for the analyser and time-of-flight technique for analysing the incident neutron energy has been designed. The window filter used consists of two beryllium blocks; Be(I) is kept at 100 K and Be(II) can have any temperature between 300 and 500 K. The spectrometer has been designed for installation on the Spallation Neutron Source, UK. It is expected to provide a continuously variable (by varying temperature of Be(II)) resolution $\Delta E/E$ from 0·75–0·94% at $E \sim 5230$ μeV. The allowed energy transfer region is -1450 μeV to $+2950$ μeV with wave vector transfer Q range of 0·82 –3·06 Å^{-1}.

Assuming 10% isotropic elastic scattering from the sample, the expected counting rates are 28–60 $\times 10^3$ counts/hr depending on whether Be(I) is at 300 or 500 K. For the two temperatures the diffuse background is expected to be less than 2% and 10% of the peak height.

A spectrometer with such characteristics will be able to provide information in space-time region not accessible with other existing spectrometers.

Appendix. Reflectivity of polycrystalline beryllium

The reflectivity of polycrystalline beryllium as a function of its thickness for neutrons having energies ~ 5230 μeV is evaluated. At 300 K, neutrons having energies between 5219 and 6400 μeV will be Bragg reflected only by $(10\bar{1}0)$ planes of Be (Hughes and Harvey 1955). The reflectivity calculation in the present context thus involves a calculation of the intensity of the neutrons, which are Bragg scattered by $(10\bar{1}0)$ planes of Be when a beam of ~ 5230 μeV neutrons is incident at right angle on a slab of thickness D_2 of polycrystalline beryllium as shown in inset of figure 6.

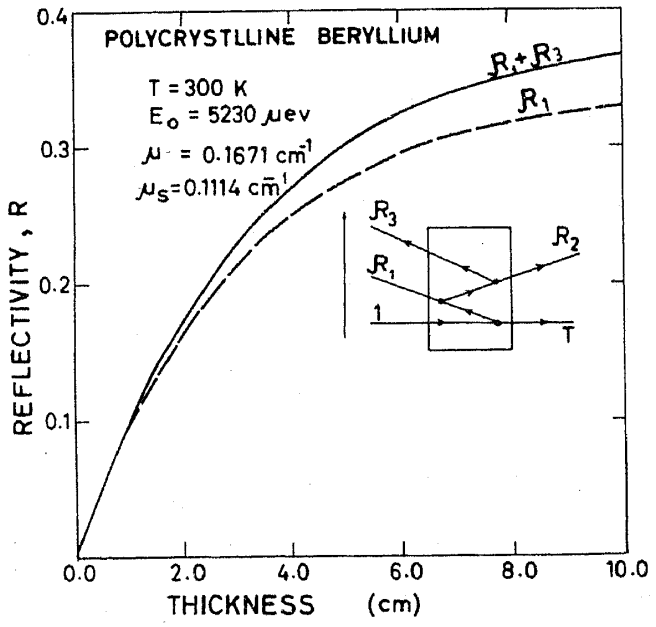

Figure 6. Reflectivity of polycrystalline Be at 300 K as a function of its thickness for neutrons having energy ~ 5230 μeV. Inset gives the geometry, for which calculations have been done. 5 cm thick Be gives a reflectivity of 30%.

Let I_0 be the intensity of the incident neutrons. Let us assume that neutrons are Bragg scattered in Be at a depth between x and $x+\mathrm{d}x$ by a scattering angle 2θ. If one integrates over the whole Debye-Scherrer ring, the intensity of the Bragg scattered neutrons is

$$I_1 = \frac{n\sigma_{\mathrm{coh}}^{\mathrm{el}}}{\sin\theta} I_0 \int_0^{D_2} \mathrm{d}x \exp[-n\sigma_T(1-\sec 2\theta)x]. \tag{A1}$$

In the energy region of interest between 5219–5236 μeV, neutrons are scattered by Be at 300 K in an angular range of 173·6–180°. In view of the large scattering angles involved, we have assumed sec $2\theta = -1$ and sin $\theta = 1$, thus getting

$$I_1 = n\sigma_{\mathrm{coh}}^{\mathrm{el}} I_0 \int_0^{D_2} \mathrm{d}x \exp(-n\sigma_T x) \tag{A2}$$

or

$$\mathscr{R}_1 = \frac{I_1}{I_0} = \left(\frac{\mu_s}{2\mu}\right)[1-\exp(-2\mu D_2)] \tag{A3}$$

where μ_s $(= n\sigma_{\mathrm{coh}}^{\mathrm{el}})$ and μ $(= n\sigma_T)$ are macroscopic Bragg scattering and total cross-sections respectively for Be at 5229 μeV. Equation (A3) gives the first order reflectivity $\mathscr{R}_1$ of Be corresponding to neutrons that emerge from the beryllium slab in the direction of the detector (figure 6) after suffering one Bragg scattering. After two Bragg scatterings, neutrons would emerge in the direction of the incident beam. However, neutrons can emerge in the direction of the detector after three Bragg scattering processes in Be as shown in figure 6. If one assumes that the second and third scattering events have taken place at depths x' and x'' respectively, the expressions for $\mathscr{R}_2$ and $\mathscr{R}_3$, the second and third order reflectivities respectively (again under back-scattering approximation) can be written as

$$\mathscr{R}_2 = \mu_s^2 \int_0^{D_2} \mathrm{d}x \exp(-\mu x) \int_0^x \mathrm{d}x' \exp[-\mu(x-x')] \cdot \exp[-\mu(D_2-x')]$$

$$\mathscr{R}_3 = \mu_s^3 \int_0^{D_2} \mathrm{d}x \exp(\mu x) \int_0^x \mathrm{d}x' \exp[-\mu(x-x')]$$

$$\times \int_{x'}^{D_2} \mathrm{d}x'' \exp[-\mu(x''-x')] \cdot \exp(-\mu x'')$$

which can be simplified to obtain

$$\mathscr{R}_2 = \left(\frac{\mu_s}{2\mu}\right)^2 \exp(-\mu D_2)[2\mu D_2 - 1 + \exp(-2\mu D_2)] \tag{A4}$$

$$\mathscr{R}_3 = \left(\frac{\mu_s}{2\mu}\right)^3 [1-\exp(-2\mu D_2)]^2. \tag{A5}$$

Reflectivities $\mathscr{R}_1$ and $\mathscr{R}_3$ of beryllium have been calculated as a function of its thickness D_2 for temperatures of 300 and 500 K. The relevant cross-sections $\sigma_{\mathrm{coh}}^{\mathrm{el}}$ and σ_T for $E \sim 5230$ μeV were obtained from BNL report (Hughes and Harvey 1955) as follows.

The measured total cross-section $\sigma_T = 0{\cdot}47$b for Be at 300 K just below the cut-off energy (5219 μeV) is mainly (= 0·45b) coherent inelastic scattering cross-section $\sigma_{\mathrm{coh}}^{\mathrm{inel}}$

as incoherent cross-section in beryllium is negligible ($\sim$ 0b) and the absorption is small ($\sigma_{abs} = 0{\cdot}02$b). It is reasonable to assume that σ_{coh}^{inel} remains 0·45b even at $E = 5230$ μeV. The value of coherent elastic (Bragg) scattering cross-section σ_{coh}^{el} for $(10\bar{1}0)$ planes of beryllium comes to 0·88b as the value of σ_T is 1·35b above the cut-off energy and 0·47b below the cut-off energy. The cross-section measurements for Be at 500 K are not available. The value of σ_{coh}^{inel} at 500 K was thus obtained to be 1·10 by extrapolating the values of σ_{coh}^{inel} at 300 and 440 K. σ_{coh}^{el} was obtained to be 0·69b using the room temperature value of 0·88 and assuming Debye temperature for beryllium to be 1000 K. This gives $\sigma_T = 1{\cdot}81$b (1·10 + 0·02 + 0·69) for Be at 500 K.

The calculated first order reflectivity $\mathscr{R}_1$ and total reflectivity $\mathscr{R}$ ($= \mathscr{R}_1 + \mathscr{R}_3$) for beryllium at 300 K is shown in figure 6. It is seen that reflectivity increases with increase in thickness D_2 of beryllium; the increase is however small beyond $D_2 = 50$ mm. The contribution from $\mathscr{R}_3$ to $\mathscr{R}$ is significant only for large thickness. For a 50 mm thick beryllium $\mathscr{R}_1 = 0{\cdot}274$ and $\mathscr{R} = 0{\cdot}30$ at 300 K. The corresponding value at 500 K are 0·170 and 0·175 respectively.

References

Alefeld B 1969 *Z. Phys.* **228** 464

American Institute of Physics Handbook 1972 (Coordinating ed D E Gray) (New York: McGraw Hill) 4-120, 9-5

Brugger R M 1965 in *Thermal neutron scattering* (ed) P A Eglestaff (London: Academic Press) p. 54

Buras B 1968 in *Theory of condensed matter* (Vienna: International Atomic Energy Agency) p. 443

Dagleish P, Hayter J B and Mezei F 1980 in *Neutron spin echo* (ed) F Mezei (Berlin: Springer-Verlag)

Dasannacharya B A 1981 *Nucl. Phys. Solid State Phys. Symp. (India)* **C24** 553

Dasannacharya B A, Goyal P S, Iyengar P K, Satya Murthy N S, Scni J N and Thaper C L (To be published)

Goyal P S, Dasannacharya B A and Satya Murthy N S 1982 in *Neutron scattering*-1981 (ed) J Faber, Jr (New York: American Institute of Physics) p. 159

Goyal P S, Thaper C L and Dasannacharya B A 1983 *Nucl. Phys. Solid State Phys. Symp. (India)* **C26** (in print)

Hughes D J and Harvey J A 1955 *Neutron cross-sections BNL*-325 a report of the Brookhaven National Laboratory, USA

Iyengar P K 1964 *Nucl. Instrum. Methods* **25** 367

Iyengar P K 1965 in *Thermal neutron scattering* (ed) P A Eglestaff (London: Academic Press) p. 98

Manning G 1978 *Contemp. Phys.* **19** 505

Taylor A D 1982 *SNS/SPG/P12/82*—a report of Rutherford Appleton Laboratory, UK

Thaper C L, Goyal P S and Dasannacharya B A 1984 *Pramana* **23** 313

Windsor C G 1981 *Pulsed neutron scattering* (London: Taylor and Francis)